Membrane-Supported Liquid-Liquid Extraction – Where Do We Stand Today?

Wolfgang Riedl[1],*

Abstract

Thanks to advances in materials science and manufacturing technology, membranes are now available for stable liquid-liquid extraction processes. Rigorous calculation models can be used to calculate the membrane areas required for a specific separation task as well as to optimize the module design. Rapid tests can determine the basic suitability and kinetic parameters. Thus, the general requirements for exploiting the specific advantages of this separation technology in technical applications are fulfilled.

Keywords: Mass transfer model, Membrane-assisted liquid-liquid extraction, Membrane contactors

Received: October 25, 2020; *accepted:* January 13, 2021

DOI: 10.1002/cben.202000032

1 Introduction

Membrane contactors occupy a special position within membrane processes: instead of filtering, they passively separate two fluid phases by acting as artificial interfaces. Of the two phases involved, usually only one wets the membrane, while the other phase is retained. Together with the characteristic membrane properties, this results in a wide range of possible separation technology applications. The specific properties of membrane contactors will be demonstrated using liquid-liquid extraction as an example.

2 Development History

Membrane-supported liquid-liquid extraction was first described in depth in 1984 by Kiani et al. [1]. Since then, this technique has been described in detail time and again, e.g., in the review articles by Gabelman and Hwang [2], Pabby and Sastre [3], a special issue of the Journal of Membrane Science [4] and inclusion in the monographs of Baker [5], Cussler [6], and Melin and Rautenbach [7].

The development history of potential membrane contactor applications has always been directly related to the availability of membranes and their shape. Thus, developments in materials science were and are a strong driver for spreading this technology. As a typical mass transfer device, the preferred membrane shape for membrane contactors is tubular. However, membrane tubes are in general less suitable for research purposes, as connecting them to lab equipment and sealing them is more demanding than with flat-sheet membranes. Therefore, the first investigations were mostly carried out with flat-sheet membranes, which have been available in various forms since the second half of the last century. The materials investigated included Polypropylene (PP), Polyvinylidene Fluoride (PVDF), Polytetraflourethylene (PTFE), and Polysulfone (PSU). Inorganic materials (ceramics) were not used initially.

The first technically available membrane contactors were produced from tubular PP membranes (3M/LiquiCel). Manufactured as hollow fibres (with diameter < 300 µm) and packed as bundles, such devices provide high volume-specific exchange surfaces of up to 30 000 m^2m^{-3} [7]. The compact design and good availability of these membrane contactors elevated this technology to obtain first references [8] and thus increased awareness. However, the chemical and thermal stability of these membranes is limited by the materials used and especially by the challenge of cross-contamination-free cleaning of the densely packed hollow fiber bundles [9]. At the beginning of this millennium, the first membranes were manufactured from inorganic materials [10] and tested for use under demanding conditions [11]. Today, however, due to new joining and fastening techniques possible with 3D printing, membrane contactors with tubular PTFE membranes have recently become available [12]. Thus, membrane contactors and not just sole membranes can be tested and piloted under demanding boundary conditions (e.g., metal salt extraction at very low pH value) or hygienic applications (food, pharmaceuticals, consumer health) requiring high temperatures for cleaning-in-place.

[1] Prof. Dr.-Ing. Wolfgang Riedl
School of Life Sciences FHNW, Hofackerstrasse 30, 4132 Muttenz, Switzerland.
Email: wolfgang.riedl@fhnw.ch

‡English version of DOI: https://doi.org/10.1002/cite.201900070

3 Operating Principle

In principle, all porous membranes with pore sizes well below 1 µm can be used in membrane contactors. Thus, both ultra- and (fine) microfiltration membranes can be applied. In this case, however, the membranes do not 'filter', but serve as an artificial interface between two fluid phases, of which only one needs to be a liquid. Ideally, one of the two phases wets the membrane and enters the membrane pores (due to capillary forces), while the second phase does not wet the membrane (Fig. 1).

As Fig. 1 shows, the phase interface between the two liquids forms at the pore exits of the membrane on the side where the non-membrane wetting liquid phase is located.To prevent the wetting phase from entering the non-wetting phase, the latter can be put under a certain overpressure. Normally, overpressure lower than 400 mbar is sufficient for this purpose [7]. This transmembrane pressure ensures that the phase interface is immobilized even during start-up and shut-down processes at the pore exit. It is important to note that the process is not a pressure-driven membrane process, but is based on the diffusion of the component(s) passing from one fluid phase into another, driven by a difference in chemical potential.

For liquid-liquid extraction purposes, the immobilization of the phase interface at the membrane pores offers the following advantages/benefits:

- No energy input necessary to disperse one phase in the other.
- No phase separation required after extraction.
- The risk of stable emulsions forming is largely limited.
- No density difference between the liquid phases necessary (as no phase separation is required).
- Phase ratios can be freely selected in wide ranges.
- Temperatures can be different in the individual phases.

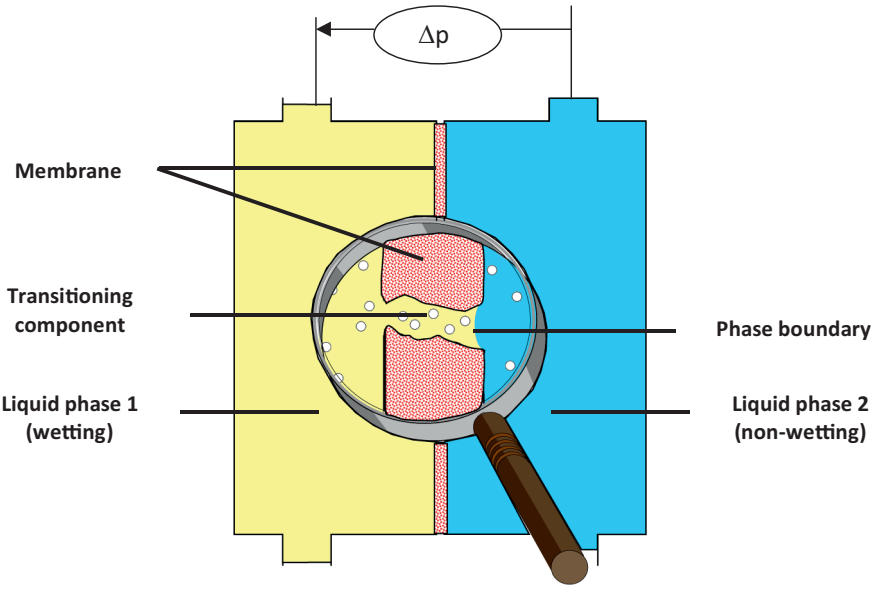

Figure 1. Basic principle of membrane-supported liquid-liquid extraction.

- Large volume-specific exchange surfaces, especially when using capillary and hollow fiber modules (up to 30 000 m^2m^{-3}).
- As long as the wetting properties of the two phases are clearly different, liquid-liquid extraction is also possible with systems forming a homogeneous liquid phase under these conditions, instead of two immiscible phases.

There is thus a fairly broad field of applications for membrane contactors in liquid-liquid extraction, as shown in Fig. 2.

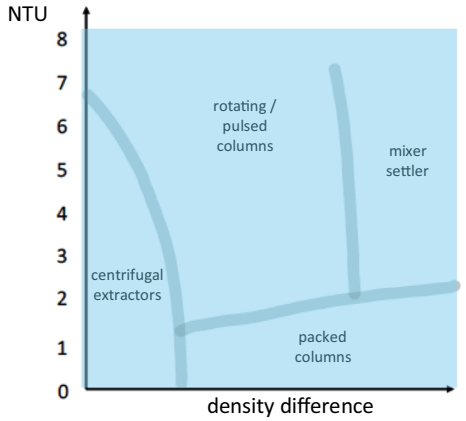

Figure 2. Operational field of membrane-supported liquid-liquid extraction in comparison to conventional extraction apparatus (based on [13]).

As Fig. 2 shows, membrane contactors generally have no restrictions with regard to the density difference and the number of theoretical steps NTU. Of particular interest, however, are applications where low density differences occur and thus the phase separation in conventional liquid-liquid extraction can only be achieved by an applied centrifugal force. This is not necessary when membrane extraction is used. As long as there are no restrictions on the membrane materials used (e.g., chemical resistance, no extractable constituents, good cleanability, etc.), the advantages of the membrane-supported liquid-liquid extraction are obvious and are therefore already at an advanced stage of development [13–21]. Multi-stage processes are also possible and have already been described [22].The membrane itself, however, generates an additional mass transfer resistance missing from conventional liquid-liquid extraction. Studies have shown that this resistance can amount to up to 40 % of the total resistance in membrane-assisted liquid-liquid extraction [23]. It is therefore desirable to keep the membrane thickness and hence the corresponding mass transfer resistance as small as possible. This is, however, difficult to reconcile with the requirements for stable operation and

solid membrane contactor construction and design. Thin-walled polymer hollow fiber or capillary membranes (with wall thickness < 150 m) therefore have an advantage in this respect over ceramic capillary membranes (with up to 3000 m wall thickness) for instance.

Finding the optimal membrane geometry is therefore a typical engineering optimization and manufacturing problem, which must also be seen in the context of the advantages of membrane-supported liquid-liquid extraction (e.g., no phase separation after extraction). Therefore, the development of new, specially manufactured membrane geometries may be beneficial. In order to reduce the number of samples required for this purpose, it is especially useful to predict the most favorable wall thickness by using rigorous mass transfer models.

4 Mass Transport Modelling

Mass transport for the component to be extracted in membrane-supported liquid-liquid extraction can be described using the classical Lewis two-film model, extended by the additional transfer step of diffusion through the membrane pores [24]. It is assumed that a laminar film is formed at the phase boundaries between liquid and membrane on both sides of the membrane. At the interface the two liquid phases are in equilibrium. Mass transfer perpendicular to the direction of flow of the two liquid phases takes place by molecular diffusion.

The driving force for the mass transfer is the difference $\Delta\mu_i$ in the chemical potentials of the transferring component i in the two liquid phases:

$$\Delta\mu_i = \mu_i^{\alpha} - \mu_i^{\beta} = RT\left(\ln a_i^{\alpha} - \ln a_i^{\beta}\right) + \bar{V}_i\left(p^{\alpha} - p^{\beta}\right) \tag{1}$$

With μ_i = chemical potential, R = universal gas constant, T = temperature, a_i = activity of component i, $\bar{V}_i$ = partial molar volume of (dissolved) component i, p = transmembrane pressure, and α, β = fluid phase index.

Prasad et al. [25] have shown that the second summand in Eq. (1) is small compared to the first term at the previous small pressure differences between the two liquid phases and can therefore be neglected. It is further assumed that the activity a_i can be expressed by a concentration c_i. The driving force in the membrane-supported liquid-liquid extraction can then be expressed approximately by the difference in the concentrations of a dedicated component passing through the two liquid phases, taking into account the distribution number Vz (derived from the Nernst distribution number N for highly diluted solutions):

$$Vz = \frac{c_{ogg}}{c_{wgg}} \tag{2}$$

Fig. 3 shows the concentration profile during the extraction of a component from the organic phase into an aqueous receiver using a hydrophobic membrane. This mass transfer model takes into account the fact that in addition to the transition component, both solvents are also extracted up to their maximum mutual solubility. These co-extractions influence the quantity of the extraction of the main component. However, if the mutual solubility of the solvents is low, this influence is negligible.

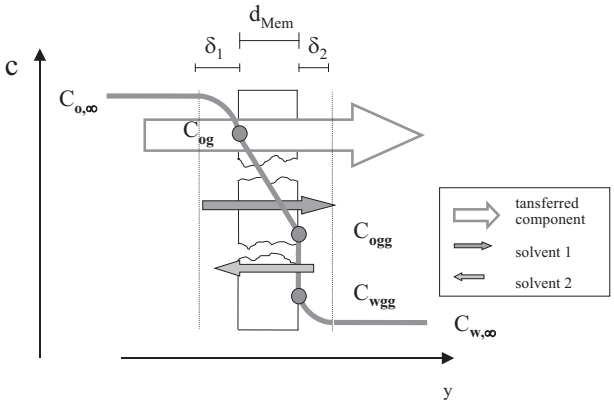

Figure 3. Concentration profile during extraction from the organic donor phase with water using a hydrophobic microporous membrane.

According to the mass transport model shown in Fig. 3, the individual transport steps can now be described quantitatively using the assumptions made. Following the general form of the description of mass transport

$$\frac{dn}{dt} = \dot{n} = K_o A(c_o - Nc_w) \tag{3}$$

with n = molar amount of transferred component, K = overall mass transfer coefficient, A = mass transfer area, N = Nernst distribution number, and c_1, c_2 = molar concentration in liquid 1 and 2, the mass transfer from the dispensing organic phase through the laminar boundary layer δ_1 can be described as:

$$\dot{n}_1 = k_o A_0 (c_o - c_{og}) \tag{4}$$

with k_o = mass transfer resistance for the transport through the organic boundary layer and A_o = organic boundary layer area.

The mass transfer through the membrane filled with organic solvent (hydrophobic membrane) can be expressed with:

$$\dot{n}_2 = k_{Mem} A_{Mem} (c_{og} - c_{ogg}) \tag{5}$$

whereas k_{Mem} = membrane mass transfer resistance and A_{Mem} = membrane area.

The mass transfer through the aqueous laminar boundary layer δ_2 is described as following:

$$\dot{n}_3 = k_w A_w (c_{wgg} - c_w) \tag{6}$$

whereas k_w = aqueous boundar layer mass transfer resistance and A_w = aqueous boundary layer area.

For all three transfer steps, the molar rate must be equal:

$$\dot{n}_1 = \dot{n}_2 = \dot{n}_3 = \dot{n} \tag{7}$$

The mass transfer resistances k_o, k_{Mem}, and k_w are defined as following:

$$k_o = \frac{D_o}{\delta_1} \tag{8}$$

with D_0 = diffusion coefficient of transferred component in organic phase and δ_1 = boundary layer thickness.

$$k_{Mem} = \frac{D_o}{\delta_{Mem}} \frac{\varepsilon}{\tau} \tag{9}$$

with ε = porosity, τ = tortuosity, and δ_{MEM} = membrane thickness.

$$k_w = \frac{D_w}{\delta_2} \tag{10}$$

With D_w = diffusion coefficient of transferred component in aqueous phase.

The diffusion coefficient D_o for diffusion through the organic boundary layer and through the hydrophobic membrane wetted by the organic solvent are assumed to be equal.

In order to make the mass transfer step through the membrane (Eq. (3)) as large as possible, the membrane mass transfer coefficient k_{Mem} (Eq. (9)) must also become as large as possible. This can be realized if the membrane has a very low thickness and/or a very low tortuosity, while at the same time having the highest possible pore ratio. Here, the membrane manufacturers are then required to generate a membrane that is optimal under these conditions and also meets the requirements for stable operation. Fig. 4 shows a SEM image of a PTFE membrane.

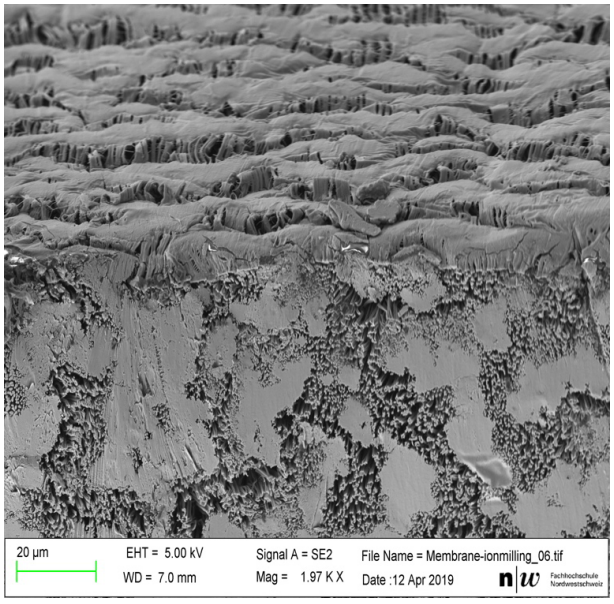

Figure 4. SEM image of a tubular PTFE membrane (front view of ion-cut wall thickness).

Fig. 4 clearly shows how the surface of the membrane has a high proportion of pores, but in the substructure of the membrane the channels branch out quickly (high tortuosity). The wall thickness of the membrane is about 200 µm, which had been shown to be (currently) the minimum possible in terms of mechanical strength and the feasiblity of installation in membrane contactors.With Eq. (7) and the assumption that all surfaces are equally large, follows:

$$A \equiv A_o = A_{Mem} = A_w \tag{11}$$

Taking Eqs. (2) and (8)–(10) into consideration, Eq. (3) can be expressed as follows:

$$\dot{n} = \frac{k_o k_{Mem} k_w}{k_{Mem} k_w + k_o k_w + k_{Mem} k_o Vz} \frac{A^3}{A^2} (c_o - Vz c_w) = \left(\frac{1}{\frac{1}{k_o} + \frac{1}{k_{Mem}} + \frac{Vz}{k_w}} \right) A (c_o - Vz c_w) \tag{12}$$

The sum of mass transfer coefficient (first bracket term in Eq. (12)) can then be combined to the over-all mass transfer coefficient K_o:

$$K_o = \left(\frac{1}{\frac{1}{k_o} + \frac{1}{k_{Mem}} + \frac{Vz}{k_w}} \right) \tag{13}$$

With this and with the volume-specific exchange area a of the corresponding membrane contactor, the desired depletion rate, the distribution number of the transferring components in the two liquid phases and the velocity in the organic phase, the contactor length or number of membrane contactors of a given length in series required for this separation task can be calculated:

$$L = \frac{v_1}{Ka} \int_{c_{1\alpha}}^{c_{1\omega}} \frac{dc_1}{c_1 - Vz c_2} = HTU \cdot NTU \tag{14}$$

with v_1= velocity of the organic discharge phase, c_1 = Concentration of the transferred components in the discharge phase and c_2 = Concentration of the transferred components in the extraction phase, and α, ω = indices for concentration at entry into (α) and exit from (ω) the apparatus.

5 Experiments

In general, models for describing mass transfer must first be provided with reliable data at central points in order to deliver reliable results: while the membrane characterization is usually reported by the manufacturers themselves as a production-technical quality feature, or, as shown above (Fig. 4), can be made accessible via (complex) imaging techniques, the diffusion coefficient of a transferring component in a liquid and at a given temperature is, for example, often unknown. Thus, experiments are inevitable.A suitable experimental setup for such a purpose is shown in Fig. 5. To carry out the experiments, first a membrane module with a known surface area and (membrane) geometry is installed. Then, the desired quantities of feed and solvent phase are placed in the two vessels and tempered if required. Figs. 6 and 7 show the test setup and membrane

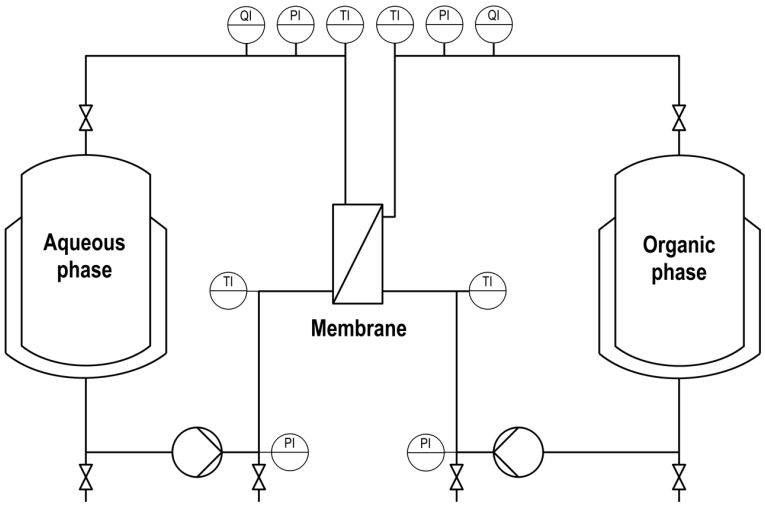

Figure 5. Scheme of experimental setup for membrane-supported liquid-liquid extractions experiments.

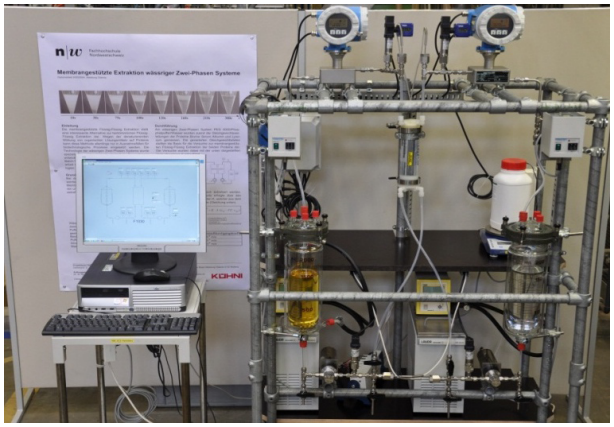

Figure 6. Test setup according to scheme of experimental set-up (Fig. 5).

Figure 7. Membrane modules used.

modules used as examples for corresponding tests (tubular PTFE membranes, $MemO_3$ GmbH).

It is benefical to start by pumping the phase that does not wet the membrane while the other phase is not yet pumped. Then, while continuing pumping, this phase is carefully placed under a certain overpressure (e.g., 100 mbar). If no phase breakthrough into the second (still empty) side of the membrane (module) can be detected after a few minutes, pumping of the second phase can be started there as well. Thus, the membrane-supported fluid-fluid contact is started (t_0).

In co-current operation mode, a typical curve is obtained for the concentration of the transferring component depending on the fluid dynamic parameters, the membrane selected and its characteristics (transfer area, material, wall thickness, porosity, tortuosity, swelling behavior) and the temperature: The concentration in the feed phase shows the course of a decay function and in the solvent phase that of a saturation function, as shown in Fig. 8.

The starting value for the concentration in the discharge phase is the weight of the passing component, for the extraction phase it is that of the initial load (usually, however, zero). The corresponding final values can be easily determined, e.g., by a shaking test under identical conditions (if necessary with phase separation by centrifugation) and are also achieved with membrane-supported liquid-liquid extraction (after sufficient time), as the membrane does not influence the final equilibrium value.

If the specific mass flow $\mathrm{d}n/(\mathrm{d}t\,A)$ is plotted against the driving force, the overall mass transfer coefficient K can be determined from the gradient of the resulting line of origin [26].

With this experimental procedure, with a manageable amount of apparatus and time, it can be shown that this technique can also be used to extract systems that tend to form emulsions without the formation of emulsions (clear extracts, clear raffinates) and thus the principle feasibility is given. If no emulsion formation occurs, the overall mass transfer coefficient K of this membrane-supported liquid-liquid extraction process can be determined by continuing the test for a sufficient time (and recording the concentration curves - see above) according to Eq. (12). Thus, the central parameter in Eq. (14) is available and process design can be carried out based on a rigorous mass transfer model with dedicated substance data.

Using the example of the extraction of ε-caprolactam from toluene into an aqueous phase, this approach resulted in the total mass transfer coefficients K shown in Fig. 9 for different (flat) sheet membranes. As Fig. 9 shows, different K values are obtained with different membranes. This can be explained on the one hand by different wall thicknesses of the membrane samples and the longer diffusion paths associated with them. On the other hand, the porosity of the membranes also has a significant influence on the overall mass transfer coefficient K: the area entering Eq. (3) is generally to be understood as the area available for mass transfer - which in this case is the area resulting from all membrane pores. As a technically accessible surface, however, it is rather unsuitable, since only the installed surface, i.e., the total geometrical surface, is used for experi-

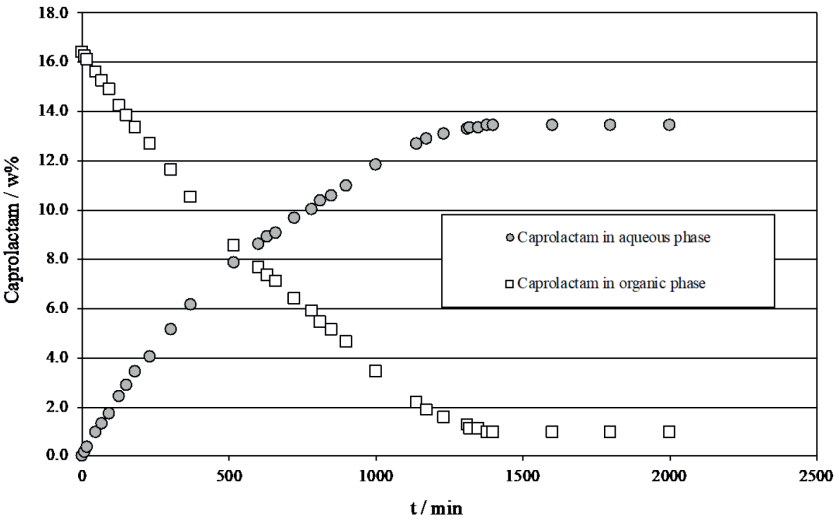

Figure 8. Temporal course of the concentration of caprolactam during membrane-supported extraction in a co-current operation mode. Direction of mass transfer organic to aqueous, circulation test in co-current mode, phase ratio 1:1, flow rates in both circuits = 200 mL min^{-1}, 25 °C extraction temperature, concentrations determined by GC analysis (multiple determination; ± 5 % accuracy).

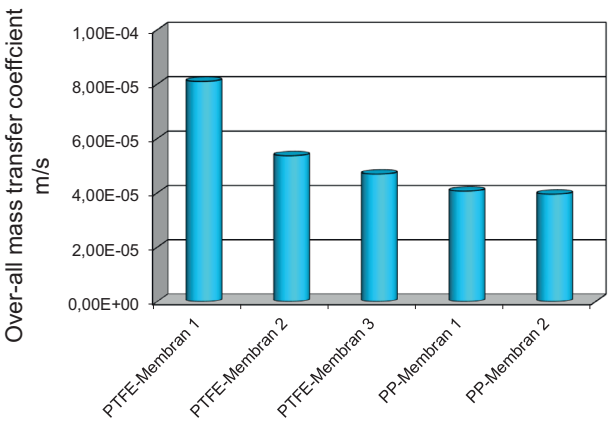

Figure 9. Experimental overall mass transfer coefficients for membrane-assisted liquid-liquid extraction of ε-caprolactam, Direction of mass transfer from organic phase to aqueous phase, co-current operation, phase ratio 1:1, flow rate in both loops = 200 mL min^{-1}, 25 °C extraction temperature.

Table 1. Properties of the membrane used for the investigations.

Membrane	Thickness [µm]	Porosity ε [%]	Tortuosity τ [–]
PTFE-Membrane 1	ca. 50	75	1.2–1.8
PTFE-Membrane 2	ca. 50	75	1.2–1.8
PTFE-Membrane 3	ca. 50	75	1.2–1.8
PP-Membrane 1	ca. 25	37	2.6–3.0
PP-Membrane 2	ca. 100	65	ca. 3

ments (for flat sheet membranes the cut-to-size total surface or for capillary and hollow fiber membranes the surface resulting from the tube geometry and length). For the same installed area, it is therefore not surprising that a membrane with a higher porosity (= higher proportion of pores, e.g, 'PTFE membrane 1' with ε = 75 %) also has higher overall mass transfer coefficients than, e.g., 'PP membrane 1' (ε = 37).

For the sake of completeness it should be mentioned that with the commonly used tubular membrane geometries (hollow fibers or capillaries with max. outside diameters < 3 mm) it is not necessary to differentiate whether the exchange surface is located more at the inner or outer pore radius outlet (and thus the inner or outer tubular radius must be used for calculation accordingly), as the wall thicknesses are usually small compared to the installed total surface.

In addition to the influence of the membrane (geometry) used on the overall mass transfer coefficient, further experiments confirmed that the membrane-supported extraction process, as can be derived from Eqs. (8)–(10), is also dependent on the selected temperature and fluid dynamics [1, 3, 23, 26].

The influence of temperature on the overall mass transfer coefficient is expressed here above all by the dependence of the diffusion coefficient of the passing components on temperature; it increases with increasing temperature. At the same time, however, solubility is also influenced, which according to Eq. (3) is also expressed in an altering driving force term.

However, this fact can then also be used to determine the usually rather less available diffusion coefficient D of a target component in a solvent at a selected temperature from tests with a well-characterized membrane (cf. Fig. 4) via the overall mass transfer coefficient K obtained from membrane-supported extraction tests [28].As expected, the influence of the fluid dynamics is shown by the boundary layer resistances forming on both sides of the membrane: with increasing flow velocity; these become smaller and thus the total mass transfer coefficient obtained becomes larger. It could be shown that a significant increase can be observed here, especially in the range of Reynolds numbers up to 300. Above this, the K value increases only slightly with an increasing Reynolds number [23].

With the dependencies of the overall mass transfer coefficient K determined in this way, further experiments based on equation 12 can be reliably predicted. Meanwhile, predictions which agree well with the data experimentally determined later under these conditions are successful with scale-up factors of more than 100 – for co-current and counter-current operation [29].

An experiment underlining the basic principles of this membrane process based on wetting/non-wetting of the membrane [23] is described below: Here the concentration of the component to be extracted -ε-caprolactam- in the aqueous donor phase and the feed phase (toluene) was adjusted differently

and the capillary rise height of the respective solution in a polypropylene hollow fibre was measured. The obtained results are shown in Tab. 2.

Table 2. Solution mixtures and their capillary rise heights (d_K = 230 µm).

Test solution (20 °C)	Concentration			
	Caprolactame [wt %]	Water [wt %]	Toluene [wt %]	Capillary rise height [mm]
1 (pure solvent)	0	100	0	0.0
2	20	80	0	0.0
3	61	29	10	19.0
4	60	20	20	31.1
4'	83	17	0	0.0
5 (Feed)	70	5	25	34.5
6	60	18	22	33.0
7	25	0	75	47.5
8	0	0	100	48.0

As Tab. 2 shows, the capillary rise height increases with increasing toluene content. At a toluene content of 10 % by weight (solution 3), the solution in the hollow PP fiber already reaches a rise height of 19 mm. At a toluene content of 20 % by weight, the measured rise height was 31.3 mm, which is hardly different from the measured rise height of the feed solution (solution 5) of 34.5 mm.

At 20 °C the ternary phase diagram, shown in Fig. 10, results for the above-mentioned substance system. As can be seen from the phase diagram, a mixture of two solutions (1 and 5 from Tab. 2) in a ratio of 6.6:1 would result in a corresponding mixing point in the homogeneous liquid phase region. A conventional liquid-liquid extraction would no longer be possible under these boundary conditions.

However, since solution 5 (toluene/ε-caprolactam) completely wets the membrane used and solution 1 (water) does not wet the membrane, a membrane-supported liquid-liquid extraction is at least theoretically possible under these conditions.

A membrane-supported liquid-liquid extraction carried out with these solutions in the chosen ratio yielded the following result (Fig. 11). As shown in Fig. 11, it was possible to extract caprolactam from the organic phase to the aqueous phase over a longer period of time. This resulted in concentrations of over 40 wt % in the aqueous phase. It was only through the co-extraction of the solvent, which, according to the phase diagram, is distributed in both liquid phases under the selected boundary conditions, that wetting of the aqueous phase also increased after about 5 h and finally led to a phase breakthrough (= end of the test).

Until then, however, it was possible to extract from the donor phase into the receiver phase without any problems. This is not possible with any other conventional liquid-liquid extraction technology and could thus be a promising approach, e.g., for yield improvement through side stream extraction.

6 Summary and Outlook

Membrane-supported liquid-liquid extraction or membrane-supported fluid-fluid contact in general represents an interesting, innovative separation process with a high degree of robustness. Objections to the use of this technology, which were previously based on chemical stability or special requirements for hygienic design (cleanability), can now only be upheld to a limited extent, particularly through the use of PTFE

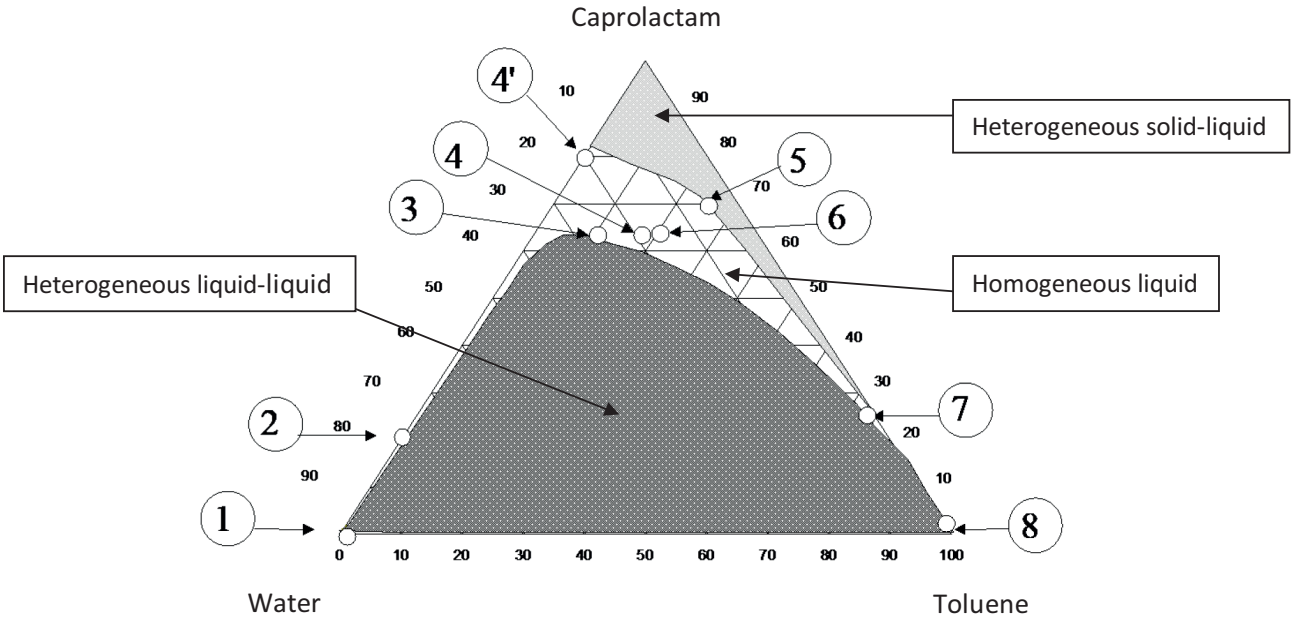

Figure 10. Sample composition; shown in the triangular diagram of the substance system water/caprolactame/toluene (20 °C).

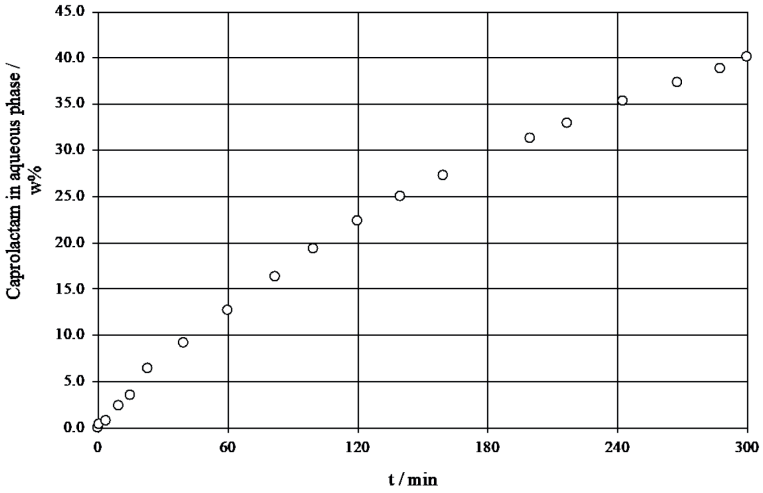

Figure 11. Concentration curve for caprolactam in water at extraction with mixing point outside the heterogeneous liquid-liquid region, direction of mass transfer organic to aqueous, co-current operation, phase ratio 6.6:1, volume flow in both circuits = 200 mL min^{-1}, 25 °C extraction temperature, donor concentration: 70 wt %, water phase initially unloaded, PP Membrane 1.

membranes. With a well-designed experimental setup, it is possible to generate mass transfer information in a short time with limited equipment requirements. Together with the availability of membrane contactors in various (standard) designs and technology that can be easily scaled-up using rigorous mass transfer models, a foundation has been laid for applying and extending the specific advantages of membrane-supported fluid-fluid contact to new areas of application. Therefore, it does not require much imagination to assume that, thanks to the engineering inventiveness, one more interesting applications will be published in the near future.

Conflicts of Interest

The authors declare no conflict of interest.

Wolfgang Riedl (*1971) graduated in chemical engineering from Friedrich-Alexander University, Erlangen-Nuremberg, in 1998 and received his doctorate there in 2002 under Prof. Dr. A. König. He subsequently worked for Kühni AG, DSM Nutritional Products GmbH and LSMW GmbH (now Exyte GmbH). Since June 2010, Prof. Riedl has been a lecturer in process engineering/chemical engineering at the University of Applied Sciences Northwestern Switzerland, School of Life Sciences, Institute of Chemistry and Bioanalytics and heads the Process Technology Center (PTC). In addition to the research and development of membrane contactors for fluid/fluid contact, one focus of his research is the scale-up of processes in the field of chemistry and renewable raw materials (bioprocess technology).

Symbols used

A	[m^2]	(mass) transfer area
a	[m^2m^{-3}]	specific transfer area
a	[–]	activity
D	[m^2s^{-1}]	diffusion coefficient
HTU	[m]	height of a transfer unit
K	[m s^{-1}]	overall mass transfer coefficient
k	[m s^{-1}]	mass transfer coefficient
L	[m]	module length
N	[–]	Nernst distribution number
NTU	[–]	number of theoretical steps
n	[mol]	molar amount
p	[bar]	pressure
R	[J $mol^{-1}K^{-1}$]	universal gas constant
T	[K]	Temperature
V	[m^3]	liquid volume
Vz	[–]	distribution number

Greek symbols

α, β	[–]	liquid phase index
δ	[–]	density thickness
ε	[–]	labyrinth factor
τ	[–]	membrane porosity
μ	[–]	chemical potential

References

[1] A. Kiani, R. R. Bhave, K. K. Sirkar, *J. Membr. Sci.* **1984**, *20*, 125–145. DOI: https://doi.org/10.1016/S0376-7388(00)81328-9

[2] A. Gabelman, S.-T. Hwang, *J. Membr. Sci.* **1999**, *159*, 61–106. DOI: https://doi.org/10.1016/S0376-7388(99)00040-X

[3] A. K. Pabby, A. M. Sastre, *J. Membr. Sci.* **2013**, *430*, 263–303. DOI: https://doi.org/10.1016/j.memsci.2012.11.060

[4] *J. Membr. Sci.* **2005**, *257*, 1–186. www.sciencedirect.com/journal/journal-of-membrane-science/vol/257/issue/1

[5] R. W. Baker, *Membrane Technology and Applications*, 3rd ed., John Wiley & Sons, Hoboken, NJ **2012**. DOI: https://doi.org/10.1002/0470020393
[6] E. L. Cussler, in *Membrane Processes in Separation and Purification*, Kluwer Academic Publishers, Dordrecht **1994**, 375–394.
[7] T. Melin, R. Rautenbach, *Membranverfahren*, 3. Auflage, Springer Verlag, Berlin **2007**.
[8] J. Schneider, *Microporous Membrane Contactors in Industrial Separation Applications*, 8. Aachener Membran Kolloquium, Aachen, March **2001**.
[9] R. Prasad, K. K. Sirkar, *J. Membr. Sci.* **1990**, *50*, 153–175. DOI: https://doi.org/10.1016/S0376-7388(00)80313-0
[10] D. J. am Ende, *Chemical Engineering in the Pharmaceutical Industry*, John Wiley & Sons, Hoboken, New Jersey, **2011**. DOI: https://doi.org/10.1002/9780470882221
[11] www.saxonia-freiberg.de/de/Saxonia/Referenzen/Foerderprojekte/MExEM_2422.html (aufgerufen am 02. Mai 2019)
[12] H. Lyko, *F&S, Filtr. Sep.* **2017**, *31 (2)*, 90–97.
[13] E. Müller, *Flüssig-Flüssig-Extraktion*, in *Ullmanns Encyclopädie der technischen Chemie Bd. 2 Verfahrenstechnik I (Grundoperationen)*, 4. Auflage, Verlag Chemie, Weinheim **1973**.
[14] W. Riedl, T. Raiser, *Desalination* **2008**, *224*, 160–167. DOI: https://doi.org/10.1016/j.desal.2007.02.088
[15] A. Dupuy, V. Athes, J. Schenk, U. Jenelten, I. Souchon, *J. Membr. Sci.* **2011**, *378*, 203–213. DOI: https://doi.org/10.1016/j.memsci.2011.05.005
[16] A. Gössi, W. Riedl, B. Schuur, *J. Chem. Technol. Biotechnol.* **2018**, *3*, 629–644. DOI: https://doi.org/10.1002/jctb.5417
[17] M. Kienberger, M. Hackl, M. Siebenhofer, *J. Environ. Chem. Eng.* **2018**, *6*, 3161–3166. DOI: https://doi.org/10.1016/j.jece.2018.05.002
[18] N. Diban, V. Athes, M. Bes, I. Souchon, *J. Membr. Sci.* **2008**, *311*, 136–146. DOI: https://doi.org/10.1016/j.memsci.2007.12.004
[19] A. K. Pabby, A. M. Sastre, *J. Membr. Sci.* **2013**, *430*, 263–303. DOI: https://doi.org/10.1016/j.memsci.2012.11.060
[20] C. Y. Tzahi, S. Gormly, E. G. Beaudry, M. T. Flynn, V. D. Adams, A. E. Childress, *J. Membr. Sci.* **2005**, *257*, 85–98. DOI: https://doi.org/10.1016/j.memsci.2004.08.039
[21] A. Gössi, F. Burgener, D. Kohler, A. Urso, B. A. Kolvenbach, W. Riedl, B. Schuur, *Sep. Purif. Technol.* **2020**, *241*, 116694. DOI: https://doi.org/10.1016/j.seppur.2020.116694
[22] R. Klaassen, P. H. M. Feron, A. E. Jansen, *Chem. Eng. Res. Des.* **2005**, *83*, 234–246. DOI: https://doi.org/10.1205/cherd.04196
[23] W. Riedl, *Membrangestützte Flüssig-Flüssig-Extraktion bei der Caprolactamherstellung*, Shaker Verlag, Aachen **2003**. DOI: https://doi.org/10.1002/1522-2640(200205)74:5<645::AID-CITE1111645>3.0.CO;2-O
[24] W. S. Ho, K. K. Sirkar, *Membrane Handbook*, Van Nostrand Reinhold, New York **1992**.
[25] R. Prasad, A. Kiani, A. Bhave, K. K. Sirkar, *J. Membr. Sci.* **1986**, *26*, 79–97. DOI: https://doi.org/10.1016/S0376-7388(00)80114-3
[26] A. König, W. Riedl, *Chem. Ing. Tech.* **2002**, *74*, 645–646. DOI: https://doi.org/10.1002/1522-2640(200205)74:5<645::AID-CITE1111645>3.0.CO;2-O
[27] M. J. Costello, A. G. Fane, P. A. Hogan, R. W. Schofield, *J. Membr. Sci.* **1993**, *80*, 1–11. DOI: https://doi.org/10.1016/0376-7388(93)85127-I
[28] W. Riedl, G. Grundler, D. Mollet, *Chimia* **2011**, *65*, 370–372. DOI: https://doi.org/10.2533/chimia.2011.370
[29] W. Riedl, *Membrankontaktoren – alter Wein durch junge Schläuche?*, ProcessNet Jahrestagung Fachgruppen Extraktion und Phytoextrakte, Hochschule für Life Sciences FHNW, Muttenz, February **2019**.

